

## Topotaxial Decomposition of Calcite-Type $\text{KNO}_3$ Crystals

S. W. KENNEDY AND W. M. KRIVEN\*

*Department of Physical and Inorganic Chemistry, University of Adelaide, Adelaide, S.A. 5001, Australia*

Received April 16, 1979; in revised form August 10, 1979

The calcite-like form of potassium nitrate,  $\text{KNO}_3$ , decomposed under the transmission electron microscope to form  $\text{KNO}_2$  which subsequently decomposed giving the high-temperature  $\beta$  form of  $\text{K}_2\text{O}$ . Two closely related orientation relations were observed for  $\text{KNO}_2$ . Referred to the four-molecule cell of  $\text{KNO}_3$ , they were  $[111]_{\text{KNO}_3} \parallel [111]_{\text{KNO}_2}$ ,  $(0\bar{1}1)_{\text{KNO}_3} \parallel (0\bar{1}1)_{\text{KNO}_2}$ ; and  $[100]_{\text{KNO}_3} \parallel [111]_{\text{KNO}_2}$ ,  $(001)_{\text{KNO}_3} \parallel (001)_{\text{KNO}_2}$ . These and a different published orientation relation for the decomposition of cadmium carbonate conform, respectively, to orientations resulting from a corresponding structural phase transformation in rubidium nitrate.  $\beta$ - $\text{K}_2\text{O}$  formed with its cube axes parallel to those of  $\text{KNO}_2$ . Both nitrate and carbonate reactions can be regarded as topotaxial. Application of the crystallographic approach to orientations and accommodation of misregistry is discussed.

### Introduction

Two different types of orientation relation have been reported for the thermal decomposition of crystalline rhombohedral carbonates  $\text{MCO}_3$ , as studied by X-ray diffraction (1-3). Under the electron microscope decomposition of  $\text{CaCO}_3$  has been shown to produce crystallites of  $\text{CaO}$  in various other orientations (4) and the participation of a poorly crystalline intermediate has also been suggested (5). The reactivity of the product, which is of technological interest, depends on these factors. Decomposition of nitrates is also a way of producing some metal oxides. There has been little crystallographic investigation of the decomposition of the corresponding rhombohedral nitrates although other aspects of the decomposition, especially under irradiation, have attracted much attention and have been reviewed (6).

The present work concerns the decomposition of postassium nitrate crystals under 100-kV electron irradiation in an electron microscope. In previous, noncrystallographic studies of the effect of electron irradiation the electrons had an energy of 1.2 MeV (7). The product of either  $\gamma$  or electron irradiation in an open system where  $\text{O}_2$  was removed was  $\text{KNO}_2$  but complete reaction was not effected (7, 8). In the present work, the new result was obtained that the reaction first produces oriented  $\text{KNO}_2$  and subsequently oriented  $\text{K}_2\text{O}$ .

Study of the decomposition of the nitrate is complementary to studies of the carbonates in that the parent carbonate and nitrate structures are essentially the same, and the product oxide or  $\text{KNO}_2$  structures are similar in both being face-centered cubic NaCl related, but changes of composition and lattice dimensions are much smaller in the nitrate. Crystallographic aspects of the reaction can also be compared with a corresponding structural transformation cubic

\* Present address: Department of Materials Science and Mineral Engineering, Hearst Mining Building, University of California, Berkeley, Calif. 94720.

$\rightleftharpoons$  calcite type in  $\text{RbNO}_3$ , studied by us (9). In a thin crystal uniformly irradiated, two possibilities might be foreseen. Either a solid solution  $\text{KNO}_3\text{-KNO}_2$  could be formed initially and would transform to the new structure, possibly with a corresponding shape change; or the product structure could be formed directly, either with a three-dimensional correspondence to the parent, or in a disordered state which might recrystallize epitaxially on the parent.

The relevant phase of  $\text{KNO}_3$  has a structure closely related to that of high calcite and can be referred to the calcite morphological cell, rhombohedral,  $a = 7.037 \text{ \AA}$ ,  $\alpha = 100^\circ 46'$ ,  $Z = 4$  (10), (Fig. 1). This corresponds to the NaCl-type cubic cell of  $\text{KNO}_2$ ,  $a = 6.66 \text{ \AA}$ ,  $Z = 4$ .  $\text{KNO}_2$  achieves the cubic structure through thermal motion of the  $\text{NO}_2^-$  ions (11).  $\text{KNO}_3$  melts at  $316^\circ\text{C}$  and  $\text{KNO}_2$  at  $440^\circ\text{C}$ .  $\text{K}_2\text{O}$  at room temperature has the antifluorite structure,  $a = 6.436 \text{ \AA}$ , in which the oxygen atoms are in fcc array but the K atoms are in simple cubic array. Another structure,  $\beta$ , was reported to exist above  $317^\circ\text{C}$ , and on the basis of X-ray powder data was considered to

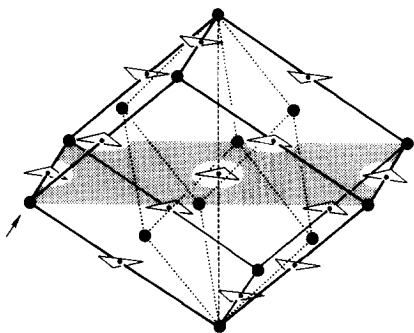


FIG. 1. The rhombohedral cell of  $\text{KNO}_3$  I. In  $\text{KNO}_2$  I this cell becomes cubic and the orientations of the anions (triangles) are randomized. In orientation relation I the trigonal axis (broken line) is parallel to a threefold axis of the cubic  $\text{KNO}_2$ . In orientation relation II the shaded (110) plane and the contained axis (arrowed) are, respectively, parallel to the corresponding plane and axis in the cubic product. The primitive rhombohedral cell (dotted lines) allows comparison with Fig. 5.

be less dense and to have a primitive cell,  $a = 12.125 \text{ \AA}$ ,  $Z = 24$  (12). The molar volume changes are  $\text{KNO}_3 \rightarrow \text{KNO}_2$ ,  $-9.7\%$ ;  $\text{KNO}_2 \rightarrow \gamma\text{-K}_2\text{O}$ ,  $-10\%$ ;  $\text{KNO}_2 \rightarrow \beta\text{-K}_2\text{O}$ ,  $+0.6\%$ . In the published powder pattern of " $\beta\text{-K}_2\text{O}$ " (12) there are no (110) or (220) reflections, the first of this type being (330).

Formally the cubic cell of  $\text{KNO}_2$  is derived from the rhombohedron of  $\text{KNO}_3$  by relative expansion along [111] and contraction in the (111) plane. As this strain does not provide a plane of fit between the structures, the product lattice is tilted with respect to the parent in a structural transformation (9).

### Experimental

Crystals of analytical-grade  $\text{KNO}_3$  were grown from aqueous solution in doubly distilled water on a carbon film on gold electron microscope grids. They were dried over silica gel. The  $\text{KNO}_3$  grew as metastable phase I (stable above  $128^\circ\text{C}$ ) or the closely related metastable phase III which immediately transforms to I in the same orientation at  $125^\circ\text{C}$  (13). They were observed under AEI EM6G and Philips EM 200 electron microscopes operated at 100 kV. The required beam intensity limited the magnifications to 20 000. In different experiments both heating and cooling stages were used but the heating stage was found to be unnecessary. The beam intensity was measured, for specific lens settings, through the exposure meter circuit in the EM 200 by placing apertures of known size in the specimen position. The intensity in the experiments was approximately  $2.10^9 \text{ electrons mm}^{-2} \text{ sec}^{-1}$ .

### Results

Crystals viewed on the {100} face immediately developed small triangular etch pits. Extinction contours then remained fixed but spread and became diffuse until the whole crystal was darkened and individual

contours were not obtainable. A sequence is shown in Fig. 2. The single-crystal diffraction pattern of  $\text{KNO}_2$  became superposed upon and gradually replaced that of  $\text{KNO}_3$ . Diffraction spots from  $\text{KNO}_2$  were initially only slightly broadened (Fig. 3), but the

orientation soon spread over about  $5^\circ$ . The crystal showed no shape change but instead became porous. The reaction reached this stage in approximately 3 min, the time depending on the beam intensity and crystal thickness.

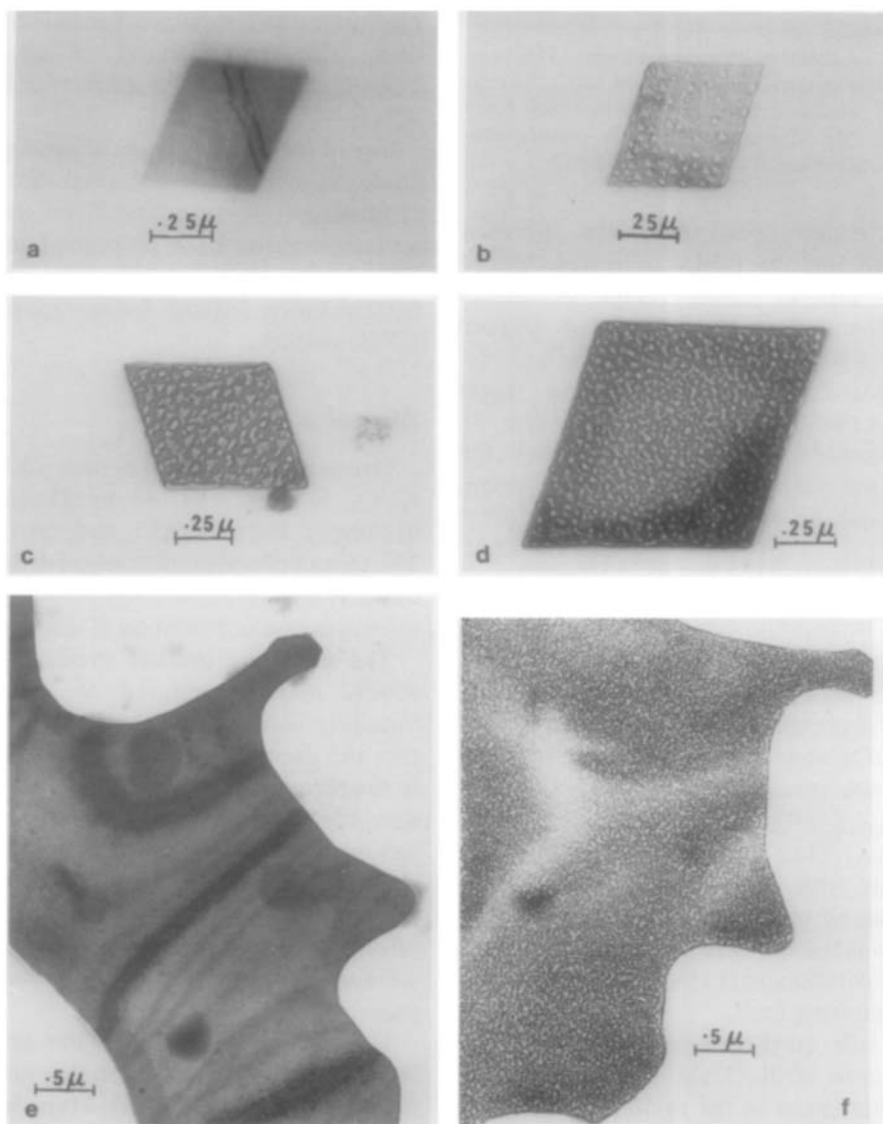


FIG. 2. (a) Typical rhombohedral crystal of  $\text{KNO}_3$  I, on  $\{100\}$  face. (b) Etch pits on same crystal after initial irradiation. (c) The subsequent state of etching on a similar crystal. (d) Etching and porosity on another crystal at the stage of formation of  $\text{KNO}_2$ . The dark area originally contained two discrete extinction contours. (e) Incipient reaction showing in extinction contours. (f) Porosity in same specimen after formation of  $\text{KNO}_2$ .

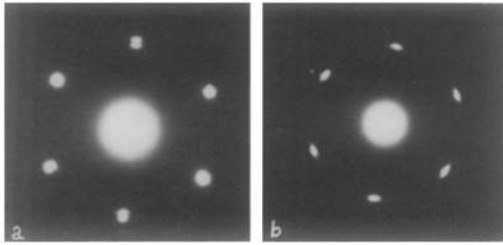


FIG. 3. (a) Electron diffraction pattern,  $[111]^*$  projection, showing coexisting  $\text{KNO}_3$  and  $\text{KNO}_2$ , and also two faint reflections between pairs of  $\{2\bar{2}0\}$   $\text{KNO}_3$  reflections. (b) Corresponding  $\text{K}_2\text{O}$  pattern after complete conversion of the  $\text{KNO}_3$  and  $\text{KNO}_2$ .

On further irradiation the porosity increased, and the  $\text{KNO}_2$  reflections spread over  $9^\circ$  around powder rings. A further diffraction pattern then appeared, aligned with the  $\text{KNO}_2$  pattern. On the  $\text{KNO}_3$   $[111]^*$  projection, the new diffraction spots matched the  $(330)$   $\beta$ - $\text{K}_2\text{O}$  spacings (Fig. 3).

In repeated experiments in which the crystal was viewed down  $[111]^*$  the orientation relations were

$$\begin{aligned} [111]_{\text{KNO}_3} \parallel [111]_{\text{KNO}_2} \parallel [111]_{\text{K}_2\text{O}(\beta)}, \\ (0\bar{1}1)_{\text{KNO}_3} \parallel (0\bar{1}1)_{\text{KNO}_2} \parallel (0\bar{1}1)_{\text{K}_2\text{O}(\beta)} \end{aligned}$$

(relation I).

When crystals were viewed down  $[100]$  and the decomposition was not taken beyond the  $\text{KNO}_2$  state a slightly different orientation was observed:  $(011)_{\text{KNO}_3} \parallel (011)_{\text{KNO}_2}$ ,  $[100]_{\text{KNO}_3} \parallel [100]_{\text{KNO}_2}$  (relation II). In this  $[111]_{\text{KNO}_3} \wedge [111]_{\text{KNO}_2} = 9 \pm 2^\circ$ . On one occasion, with heavier irradiation, giving a wide spread of diffraction spots, the orientation was the spinel twin of this, related to it by  $180^\circ$  rotation on  $(111)$ , corresponding to a single stacking fault.

On still further irradiation after the appearance of  $\text{K}_2\text{O}$  the specimen melted, crystallites grew in the melt, and the whole specimen became solid again. It then consisted of good crystallites, as shown by their extinction contours. The diffraction pattern consisted of spotty powder rings corresponding to  $\text{K}_2\text{O}$ .

At the earlier stage, before the pattern of  $\text{K}_2\text{O}$  appeared, the  $[111]^*$  projections of the  $\text{KNO}_3$  contained reflections at one-third the  $\{2\bar{2}0\}^*$  spacings on rows joining the adjacent  $\{2\bar{2}0\}$   $\text{KNO}_3$  reflections and consistent with a superlattice. They were not observed in other orientations and the lifetime of the specimen did not permit further manipulations. Such a pattern could indicate ordering in an intermediate solid solution of  $\text{KNO}_2$  in  $\text{KNO}_3$ .

Use of the cooling stage, at approximately liquid  $\text{N}_2$  temperature, showed that the rate of formation of crystalline  $\text{KNO}_2$  depended on temperature, since no porosity appeared after 15 min, but thereafter the diffraction pattern faded without being replaced by a  $\text{KNO}_2$  pattern.

## Discussion

Orientation relation I between  $\text{KNO}_3$  and  $\text{KNO}_2$  is that reported by Dasgupta for decomposition of  $\text{MgCO}_3$  and  $\text{FeCO}_3$  (1, 2). The spread of orientation, observed by X-ray diffraction in those carbonates, was sufficient to encompass our relation II also.

The etch pits initially produced on the  $\text{KNO}_3$  may correspond to dislocations. Similarly Thomas and Renshaw (14) showed that the decomposition of calcite originated in the formation of dislocation etch pits, and also concluded from consideration of dislocations that  $\{10l\}$  and  $\{100\}$  planes were significant in the mechanism. Our "superlattice" reflections suggest that as radiation effects spread through the crystal an ordered solid solution was formed as an intermediate stage.

Relation II is similar to the orientation (termed A) in the corresponding martensitic transformation cubic  $\text{KNO}_2$  I type  $\rightleftharpoons \text{KNO}_3$  I type in  $\text{RbNO}_3$ , in which  $\Delta V < 1\%$  ( $\text{BaCO}_3$  shows the same structure change). The difference is that in the transformation a  $\{100\}$  plane and a  $\langle 100 \rangle$  edge remain nearly unrotated, while in the decomposition a

{110} plane and its  $\langle 100 \rangle$  edge, respectively, remain parallel. This orientation brings respective [310] directions nearly into coincidence, and incidentally the densely packed [100] rows also. These [310] directions are very close to unextended vectors of the lattice strain for the decomposition. When unextended vectors are even approximately aligned, there is relatively good fit between the structures. As the densely packed row [100], though not an unextended vector, changes little in periodicity from 7.037 to 6.66 Å, a ratio of 0.946, it also can be preserved.

The structural accommodation can be considered in more detail. It has been suggested that the structure-change part of such reactions is martensitic (15). In applying this term one should recall that the characteristics of a martensitic transformation are an interfacial plane which is undistorted when averaged over many unit cells, and a consequent regular shape change; and that these are the criteria for recognition of it. On the other hand one of us has argued that where the array of one set of atoms is maintained though deformed through a three-dimensional correspondence in a topotaxial reaction, the problem of maintaining coherency between the structures is similar to that in a martensitic transformation; and has shown that under some conditions martensite theory would be consistent with the observations of the later stages of precipitation of twinned spinel from oxide (16). We have also suggested that where there is some diffusional adjustment the tendency for minimal diffusion will ensure that the orientation relation will be close to that produced by a martensitic mechanism (17). Where a structural correspondence (deformation) links the structure types, martensite theory may therefore indicate the optimal orientation and interface. In the  $\text{RbNO}_3$  transformation under appropriate conditions martensite theory accounted for the observations (9). In

the present work we made similar martensite calculations for the decomposition  $\text{KNO}_3 \rightarrow \text{KNO}_2$  (18) by the stereographic method (19, 20). The principle is that there would be average matching of the lattices if two unextended vectors retained their directions, thus defining a plane of fit. The unextended vectors, however, lie on cones which have different semiapex angles in parent and product, in this case  $54^\circ$  and  $46^\circ$ , respectively. If the product lattice is formed in an orientation which preserves one unextended vector another is brought into coincidence with its parent vector by further displacements analogous to slip. These constitute the lattice-invariant shear (LIS). The LI system which gave a mathematical solution for the present problem was (100)[011]. Though less common for a NaCl structure this is a slip mode of the rhombohedral structure. The predicted orientation relation was within  $0.6^\circ$  or relation II. This at least proves that of the observed orientation corresponds to optimum fit, and that diffusive displacements of ions are not essential. All the volume change would be provided by shrinkage normal to the optimum interfaces which for the present reaction were calculated to be of approximately {310} types. In general, this shrinkage would facilitate microcracking and hence porosity, except in a special case in which the optimal interface was parallel to the reacting face and participation of the symmetry equivalents was inhibited, for example, by the greater stresses. If this case could be realized, porosity would be at a minimum.

There is less structural reason for relation I in the nitrate. It is the orientation of maximum misregistry both in and normal to [111], the relative periodicities being 0.868 and 1.197, respectively. Relations I and II were obtained from different initial orientations of the parent crystal. In each case the plane of irradiation (normal to the beam) was preserved unrotated. While the difference between these orientations is not great, it

indicates less rigorous structural control than in a transformation.

The further decomposition, which was not to the room temperature phase of  $K_2O$ , confirms that there is a further phase,  $\beta$ , with at least approximate composition  $K_2O$ , with the previously reported interplanar spacings. The observed orientation then implies that the  $\beta$ - $K_2O$  grew epitaxially or topotaxially aligned to the  $KNO_2$ . This is consistent with the negligible molar volume change between  $KNO_2$  and  $\beta$ - $K_2O$ .

The structure of  $\beta$ - $K_2O$  is not known. In  $\gamma$ - $K_2O$  the packing is of CsCl type. While the 11% change of molar volume to  $\beta$ - $K_2O$  is less than  $\Delta V$  in CsCl  $\rightarrow$  NaCl-type transformations (16%), it is large enough to suggest that the structure of  $\beta$ - $K_2O$  may be related to NaCl, the K atoms then being in fcc array. This concept would imply a change of bonding. It would explain the structural alignment to the fcc array in  $KNO_2$ .

In carbonates the dimensional changes differ from those in the nitrate.  $V_{oxide}/V_{carbonate} \approx 0.40$ – $0.45$ , and  $[111]$  is nearest to an unextended vector, the length ratio being in the range 0.97 in  $MgCO_3$  to 1.0 in  $CdCO_3$ . There is, however, a gross misregistry in the  $(111)$  plane, the relative periodicity being 0.65 in  $MgCO_3$ . The structural reason for Dasgupta's relation is therefore based on a one-dimensional fit.

In a recent X-ray study of the decomposition of  $CdCO_3$  (3) the type I relation was not observed. The observed relation was previously referred to the hexagonal cell,  $Z=6$ , of  $CdCO_3$ . This masks the correspondence between the NaCl-related cells. Restated with reference to the four-molecule cells, the orientation relation was  $(001)_o || (10\bar{1})_c$ ,  $[\bar{1}40]_o || [111]_c$  (where o refers to CdO and c to  $CdCO_3$ ), with a spread of orientation (Fig. 4). This puts  $\{110\}_o$  planes nearly parallel to  $\{100\}_c$  faces (within  $9^\circ$ ). The relative areas of these planes is 0.81, a substantial decrease, but much less than the volume ratio, and without gross dimensional

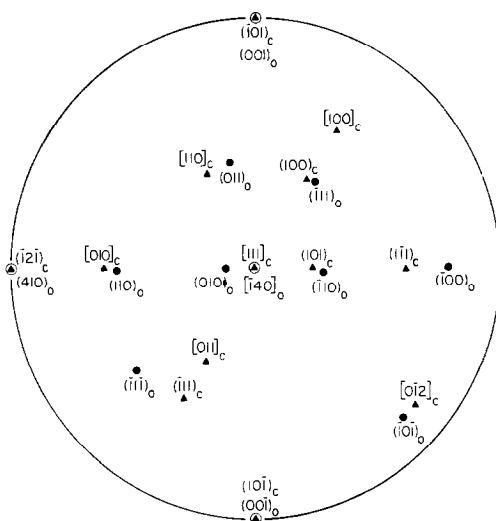


FIG. 4. Stereogram of the reported orientation relation between CdO and  $CdCO_3$  (3) referred to the four-molecule rhombohedron of  $CdCO_3$  which corresponds to the cell of CdO. Triangles denote carbonate, filled and open circles oxide.

changes in either direction. Epitaxial growth in such an orientation would therefore be relatively favored. The 19% decrease in area would still necessarily lead to porosity. The mechanism of the rearrangement for this orientation was not otherwise explained (3). There is, however, again a close analogy with the  $RbNO_3$  I  $\rightarrow$  II transformation, suggesting more than a simply epitaxial control of orientation. When  $RbNO_3$  transformed nonmartensitically (9) under conditions which permitted limited diffusional adjustment the orientation relation (termed B) was similar to that in  $CdCO_3$ . This type of orientation relation is also derivable from one of a set of correspondences for changes of first coordination proposed by Kennedy (21). In the correspondence as applied to  $CdCO_3$ ,  $(111)_c$  planes deform by relative expansion along  $[10\bar{1}]_c$  and shear slightly along  $[10\bar{1}]_c$  to become square nets of cubic  $(100)$  planes and as a consequence anions are nondiffusively displaced into their new octahedral sites (Fig. 5). The correspondence is  $(111)_c \rightarrow (100)_o$ ,

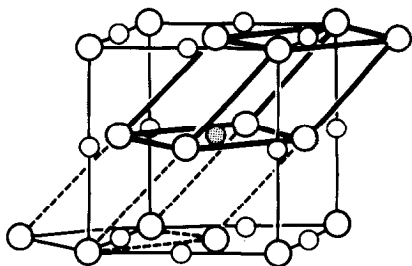


FIG. 5. The NaCl structure of CdO. In the orientation relation discussed for  $\text{CdCO}_3$  the primitive cell shown in Fig. 1 deforms to become the subcell here heavily outlined and the anion (shaded circle) is displaced from the center to the face of the subcell.

$(10\bar{1})_c \rightarrow (001)_o$ ,  $[01\bar{1}]_c \rightarrow [011]_o$ ,  $[101]_c \rightarrow [110]_o$ . This is similar to the observed orientation relation. This general type of deformation has been introduced elsewhere (17) and will be discussed in connection with the  $\text{RbNO}_3$  transformation (S. W. Kennedy, W. M. Kriven, and E. W. Courtenay, in preparation). The actual orientation depends on the best matching of planes within the correspondence. In the carbonate no complete average matching is available because of the large contraction, but the contiguity of  $(110)_o$ ,  $(100)_c$  approaches the best match available.

In the decomposition of  $\text{CaCO}_3$  under intense irradiation in the electron microscope (4), the formation of differently oriented acicular crystallites of CaO may correspond to recrystallization of the imperfect initial oxide. This initial porous intermediate, having poor thermal conduction, could reach high surface temperatures which by promoting diffusion would facilitate recrystallization, and whisker crystals frequently grow from less perfectly crystallized material, e.g.,  $\text{AgNO}_3$  or  $\text{NH}_4\text{Br}$  (22).

Since the orientation of  $\text{KNO}_2$  from the nitrate and of CaO from the decomposition of  $\text{CdCO}_3$  are, respectively, similar to two different orientations produced by the analogous phase transformation in  $\text{RbNO}_3$

they correspond to strong structural control, consistent with three-dimensional correspondences.

### Acknowledgments

S.W.K. thanks Dr. J. D. C. McConnell for hospitality and use of the microscope at the Department of Mineralogy and Petrology, Cambridge University, England, in 1969 when the decomposition was observed incidentally to other work but not further investigated. The present work received support from the Australian Research Grants Committee.

### References

1. D. R. DASGUPTA, *Indian J. Phys.* **38**, 623 (1964).
2. D. R. DASGUPTA, *Ind. J. Earth Sci.* **1**, 60 (1974).
3. N. FLOQUET AND J. C. NIEPCE, *J. Mater. Sci.* **13**, 766 (1978).
4. K. M. TOWE, *Nature (London)* **274**, 239 (1978).
5. D. BERUTO AND A. W. SEARCY, *Nature (London)* **263**, 221 (1976).
6. V. V. GROMOV, *Russ. Chem. Rev.* **43**, 79 (1975); *Usp. Khim.* **43**, 201 (1974).
7. C. HENNIG, R. LEES, AND M. S. MATHESON, *J. Chem. Phys.* **21**, 664 (1953).
8. H. B. POGGE AND F. T. JONES, *J. Phys. Chem.* **74**, 1700 (1970).
9. S. W. KENNEDY AND W. M. KRIVEN, *J. Mater. Sci.* **11**, 1767 (1976).
10. K. O. STORMME, *Acta. Chem. Scand.* **23**, 1625 (1969).
11. K. O. STORMME, *Acta Chem. Scand.* **24**, 1475 (1970).
12. PH. TOUZAIN, F. BRISSE, AND M. CAILLET, *Canad. J. Chem.* **48**, 3358 (1970).
13. S. W. KENNEDY, *J. Cryst. Growth* **16**, 274 (1972).
14. J. M. THOMAS AND G. D. RENSHAW, *J. Chem. Soc. A*, 2058 (1967).
15. J. C. NIEPCE, M. TH. MESNIER, AND D. LOUËR, *J. Solid State Chem.* **22**, 341 (1977).
16. S. W. KENNEDY, *J. Mater. Sci.* **9**, 1557 (1974).
17. S. W. KENNEDY, *J. Solid State Chem.* **34**, 31 (1980).
18. W. M. KRIVEN, Ph.D. thesis, Adelaide (1976).
19. M. S. WECHSLER, D. S. LIEBERMAN, AND T. A. REID, *Trans. Amer. Inst. Mining Met. Eng.* **197**, 1503 (1953).
20. W. L. FRASER AND S. W. KENNEDY, *Acta Crystallogr. Sect. A* **30**, 13 (1974).
21. S. W. KENNEDY, *J. Mater. Sci.* **9**, 2053 (1974).
22. S. W. KENNEDY, J. H. PATTERSON, R. P. CHAPLIN, AND A. L. MACKAY, *J. Solid State Chem.* **10**, 102 (1974).